Scientific Research Publishing

Open Journal of Fluid Dynamics, 2019, 9, 49-62
http://www.scirp.org/journal/ojfd
ISSN Online: 2165-3860
ISSN Print: 2165-3852

Design of a Centrifugal Compressor for Micro Gas Turbine: Investigation of Scaling and Tip Clearance Effects

Dario Barsi, Alberto Bottino, Andrea Perrone, Luca Ratto, Pietro Zunino

Department of Mechanical, Energy, Management and Transportation Engineering, University of Genova, Genova, Italy
Email: dario.barsi@unige.it

How to cite this paper: Barsi, D., Bottino, A., Perrone, A., Ratto, L. and Zunino, P. (2019) Design of a Centrifugal Compressor for Micro Gas Turbine: Investigation of Scaling and Tip Clearance Effects. *Open Journal of Fluid Dynamics*, **9**, 49-62.
https://doi.org/10.4236/ojfd.2019.91003

Received: January 2, 2019
Accepted: February 18, 2019
Published: February 21, 2019

Abstract

The aim of this paper is to investigate the design in similarity of a centrifugal compressor for micro gas turbine and the related scaling effects on performance using CFD investigations. This work is part of a research project carried out by the Department DIME of the University of Genova, with the purpose of investigating the performance of a micro gas turbine in the change from 100 kW electrical output to 250 kW, while maintaining the compressor pressure ratio and geometry in similarity. The first part of the work focuses on the comparison between the original and the scaled machine, while the second part of the study deeply investigates the tip gap effect in the new configuration. The aim is to provide information about the performance of the compressor designed in geometrical similarity and to evaluate the tip gap height impact. From the efficiency point of view, the scaled-up machine has higher efficiency (up to 1.4% increment in design conditions) keeping the same technological limit for impeller manufacturing. However, the variation of tip gap height in the range 0 ÷ 1 mm strongly affects this parameter, leading to 10% alteration in design conditions between the ideal and worst case. The results, both in terms of overall performance and flow fields, are widely discussed in order to obtain simple yet reliable correlation for preliminary design.

Keywords

Centrifugal Compressor, Scaling, Tip Gap, CFD

1. Introduction

In recent years, MGT have been more and more used as cogeneration systems for distributed power generation; this is caused by their good performance,

coupled with their compactness and low cost [1]. Because of MGT's small size, the machines have usually a radial configuration (instead of an axial one), preferred for its high power-to-weight ratio which leads to a more compact system. This justifies the large application of centrifugal compressors and the interest in their study in order to achieve better performance having a better understanding of phenomena within the machine. The flow structures in centrifugal compressors are considered amongst the most complex in turbomachinery [2]. This is caused by the strong change in direction which the flow has to perform and the high pressure ratio per stage; this leads to a strong interaction between main flow and leakage flow in the tip gap region, with the creation of complex vortexes. For this reason, the study of tip gap influence on both performance and flow field is interesting and it has been widely analysed in literature by several works ([3] [4] [5]). This paper aims to relate performance and internal aerodynamics, investigating the machines flow fields to corroborate the global parameters variation (e.g. total to total efficiency and pressure ratio) due to tip gap height.

Scaling effects, which refer to the study of performance of turbomachinery designed in geometrical similarity, are another topic which has been widely discussed because of its practical application; indeed, this method allows designing machines of different power, maintaining the same components geometry and the same thermodynamic cycle. Head and Visser [6] have found relationships predicting MGT performance when scaled, taking into account each component of the system. In general, scaled up machines have better performance than the original ones; in centrifugal compressors, this effect is due to several reasons such as Reynolds number variation [7] and scale effect in the tip gap region. This work shows the impact of Reynolds number variation due to the increase in dimensions keeping the same percentage tip gap height and studies independently the tip gap contribution to machine behaviour.

2. Compressor Description and Scaling Up

The compressor studied in this work has been developed by DIME in a research project related to the multidisciplinary optimization of several components of a MGT. The preliminary geometry, obtained by employing a classical one-dimensional and then two-dimensional design procedures [8], has been optimized by using an artificial neural network coupled with a genetic algorithm with the purpose of minimizing an objective function linked to aerodynamics losses and mechanical stresses; the results of this work are widely presented in [9] and [10]. In the following, the main characteristics of the compressor are summarized. The original compressor has been designed in order to be suitable for a MGT application of 100 kWe. In order to obtain a new machine able to be employed within a MGT application with a net electric power of 250 kWe, the first step of this work was to scale up the compressor by means of classic approach. Using the correlations discussed by Dufour *et al.* [11], a scaling up of the machine was performed imposing the geometrical similarity and keeping the

same values of total quantities at the inlet; this led to a scaled machine with the same velocity triangles of the original one, maintaining the same thermodynamic cycle overall parameters. Referring to Dufour *et al.* scaling parameters, indicating with superscript b and s the baseline and scaled quanties respectively, we obtain:

$$\alpha = \frac{p_{t1}^{s}}{p_{t1}^{b}} \quad \beta = \frac{RT_{t1}^{s}}{RT_{t1}^{b}} \quad \lambda = \frac{\dot{m}^{s}}{\dot{m}^{b}} \tag{1}$$

where p_{t1} and T_{t1} are the inlet total pressure and temperature, R is the gas constant and $\dot{m}$ is the mass flow rate. Since the inlet total conditions are the same for baseline and scaled machines $(\alpha = \beta = 1)$, while the mass flow rate scaling factor is equal to 2.5, the geometrical length scaling factor provided by [10] is:

$$\frac{D^{s}}{D^{b}} = \alpha^{-\frac{1}{2}} \beta^{\frac{1}{4}} \lambda^{\frac{1}{2}} = 2.5^{\frac{1}{2}} \cong 1.58 \tag{2}$$

The main parameters of these two machines are listed in **Table 1**; geometrical parameters variations are caused by appropriate scaling coefficients given by similarity laws. In **Figure 1**, a 3D render of the machine is presented, while in **Figure 2** there is an explicative dimensional comparison between the two compressors in the meridional channel of original and scaled up impeller.

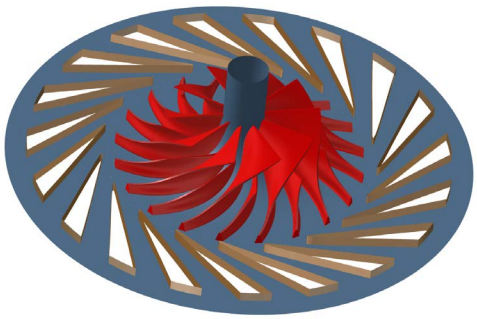

Figure 1. 3D rendering of the centrifugal compressor.

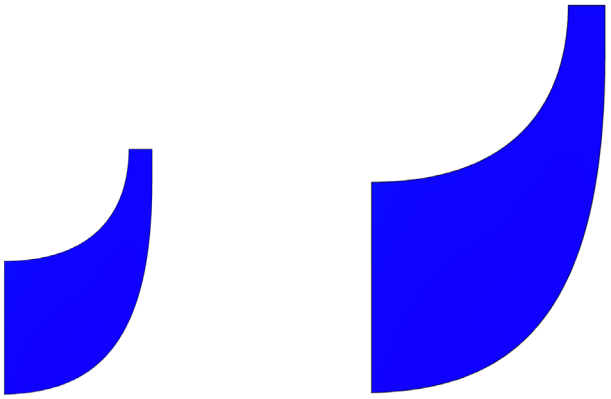

(a) (b)

Figure 2. Original (a) and scaled up (b) impeller meridional channel.

Table 1. Original and scaled compressor target main parameters.

Quantity	Original (100 kW_e)	Scaled up (250 kW_e)
Number of impeller blades	10 + 10	10 + 10
Number of diffuser blades	19	19
Impeller exit radius [mm]	64	101
Design efficiency [%]	84	84
Total to total pressure ratio [-]	4.6	4.6
Design mass flow rate [kg/s]	0.74	1.85
Rotation speed [rpm]	75,000	47,450

The tip gap was scaled, in this first analysis, using two different approaches: the first, maintaining the absolute value of the tip gap, equal to 0.2 mm, intended as a lower technological limit for impeller manufacturing; the second one, scaling the value of the tip gap itself, thus maintaining the same relative gap (intended as scaled percentage on the height of the blade), thus equal to 0.32 mm for this case. After this preliminary analysis, a detailed investigation about tip gap height effects on machine performance have been carried out. To achieve this result, different values of the tip gap height have been simulated. In this analysis, the geometry of the meridional channel and of the blades has not been modified with respect to the result of the scaling up process illustrated above. Therefore, the geometries investigated differ from each other only for the value of the tip gap height. In this second analysis, in addition to the ideal case, represented by a value equal to zero, five values of the tip gap height, with 0.2 mm pitch, were investigated, up to a maximum value of 1 mm, taken as the upper limit for the construction of the machine.

3. Mesh Generation and CFD Analysis

The computational mesh was generated in Autogrid [12] using a structured multi-block mesh with hexahedral elements. Impeller and diffuser blocks were realised separately and then conveniently coupled. The mesh has about 2 millions of elements, 1.4 for the impeller and 0.6 for the diffuser respectively. The total amount of cells has been chosen based on a grid dependency analysis carried out on the preliminary configuration, with particular focus on shock wave losses [8]. In **Figure 3**, the midspan blade to blade view is presented for rotor and stator. The first cell height has been computed in order to obtain a y^+ value of about unity. In order to improve the results accuracy, the mesh quality, in terms of orthogonality and skewness angles, was optimized though the internal Autogrid algorithm. In order to analyse the tip gap effects, rotor meshes were realised for every geometrical configuration modifying the gap height in Autogrid and keeping the same other mesh parameters; then, every rotor has been coupled with the same diffuser in IGG to simulate the full domain. This process

led to have meshes with the same grid except for the tip gap height. CFD simulations were performed using FINE/Turbo [12]; a steady RANS approach was used, modelling the turbulence with the two equations model SST (Shear Stress Transport) [13]. Total flow conditions, absolute angles and turbulence parameters were set at the inlet, while mass flow rate was imposed at machine outlet. No-slip condition was imposed at solid walls and periodicity condition was applied both on rotor and stator to couple periodic surfaces. The rotor/stator interface was modelled through the mixing plane approach.

In order to obtain the performance curve of the original and scaled up machines, several operating conditions were simulated, varying the mass flow rate. Using this outlet boundary condition, the solver adjusts the pressure ratio to satisfy continuity equation. Choking is detected when the inlet mass flow rate mismatches the outlet condition, so the flow rate is decreased in order to obtain a converged simulation. Stall is considered when the main machine parameters present unacceptable oscillations during simulations, leading to not converged calculations when the mass flow rate is strongly decreased. More precise considerations could be done using unsteady investigations near stall region, but this is out of the primary scope of this work, since it aims to provide simple yet useful indications in first guess design procedure.

4. Results

4.1. Scaling-Up

In the following, the results obtained for scaled up machines are presented. In the first part, the Reynolds effect on scaling methods is presented, while in the second part, the effect of tip gap height on performance curves is presented, with a detailed investigation on flow field behavior. The first application concerned, as mentioned, the analysis of the scaling effects of the machine using absolute scaling and relative scaling of the tip gap height. These effects are first investigated by comparing the characteristic curves of the machines, in terms of efficiency and in terms of compression ratio. In **Figure 4** the comparison between original and scaled up compressors in terms of total-to-total isentropic efficiency is presented.

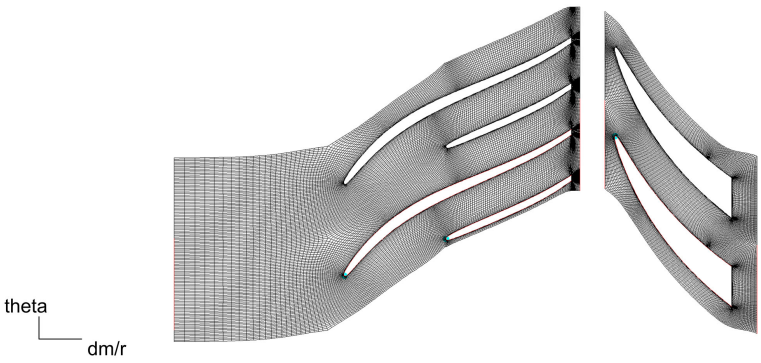

Figure 3. Blade to blade mesh for impeller and diffuser row.

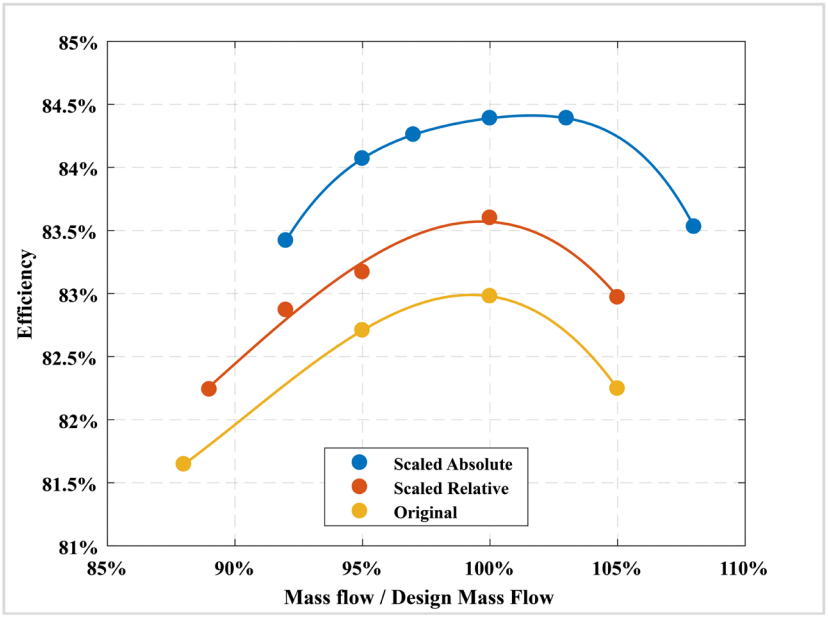

Figure 4. Total to total efficiency curves of original and scaled compressors.

As expected, the scale effect leads to an increase in efficiency in all operating points of the curves of larger machines. In the case of absolute scaling, the efficiency curve shows a flatter behavior in the central zone, resulting in a high efficiency value in a wide range of flow rates, while the curve of the relative scaling machine has a shape very similar to that of the original one, simply translated upwards. From the extension of the operating range point of view, it is noted how the machine with relative scaling presents the point of surge moved to the right compared to that of the original machine, while the chocking point is roughly obtained for the same value of mass flow rate. In the case of the absolute scaled machine, instead, both extreme points of the curve are translated to the right, with amplitude of the operating range, in terms of variation in mass flow rate, almost equal to that of the original machine. For total to total pressure ratio β_{tt}, shown in Figure 5, the absolute scaled machine presents values, for all the simulated operating conditions, higher than those of the original machine, with a shift towards the right, and therefore of the flow values corresponding to the surge and chocking, while the curve obtained for the relative scaled machine appears to be almost identical with that of the original one.

This means that the effect of the Reynolds number appears to be for this second case, marginal as regards the value of the pressure ratio.

4.2. Tip Gap Height Variation

4.2.1. Global Performance

The effects of the tip gap height was investigated by simulating different values of this size, from the ideal case, with zero gap, up to a value of 1 mm, using a 0.2 mm pitch. Figure 6 shows the total to total efficiency curves as a function of the mass flow rate, for different operating points. As expected, a gradual reduction

in efficiency is obtained with an increase in the tip gap height.

While the ideal case has a maximum efficiency of around 86.5%, the value is reduced of about 10 percentage points for 1 mm condition. Furthermore, there is a gradual decrease in both the value of the surge and chocking mass flow rates, and a strong reduction in the amplitude of the operating range. From Figure 6, it is also noticed that the design mass flow rate, equal to 1.85 kg/s, can be obtained at most with a height value of the tip gap of 0.6 mm. For higher values, in fact, the operating curves exist for lower values of the mass flow rate. Similar considerations can also be made for the total to total compression ratio, shown in Figure 7, which presents a gradual decrease with increasing tip gap height values.

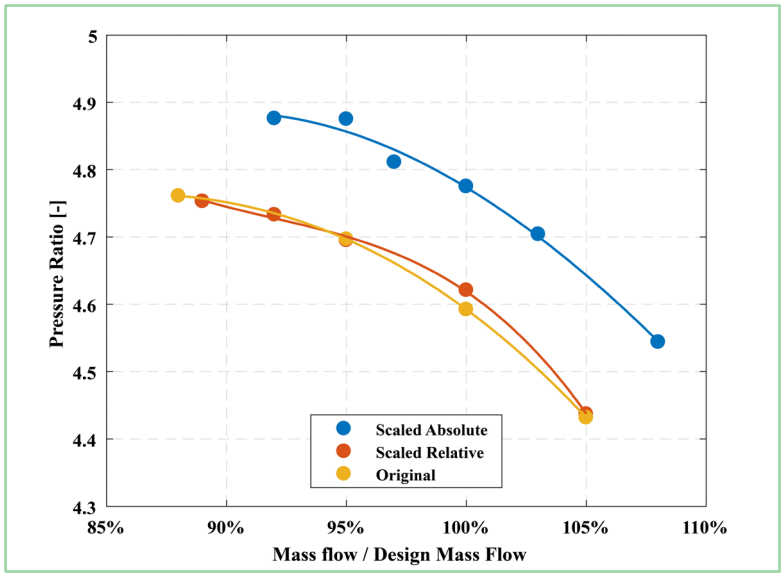

Figure 5. Pressure tario curves for original and scaled compressors.

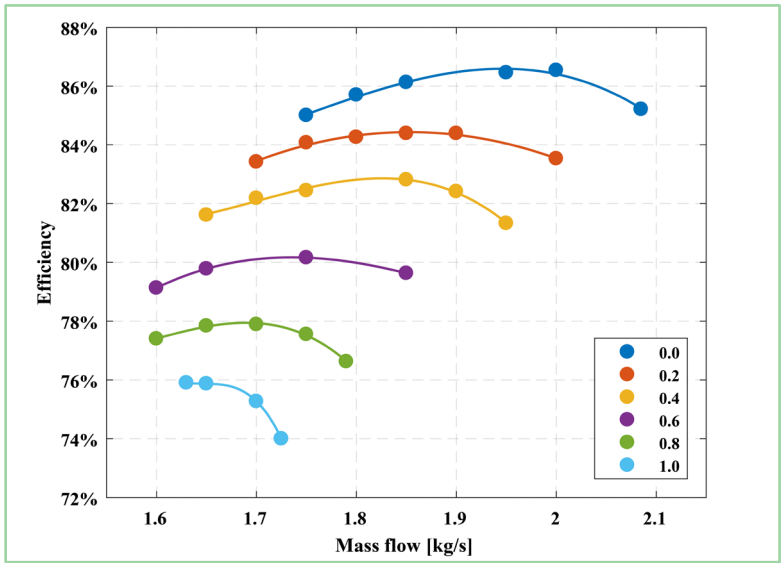

Figure 6. Total to total efficiency curves for several tip gap heights.

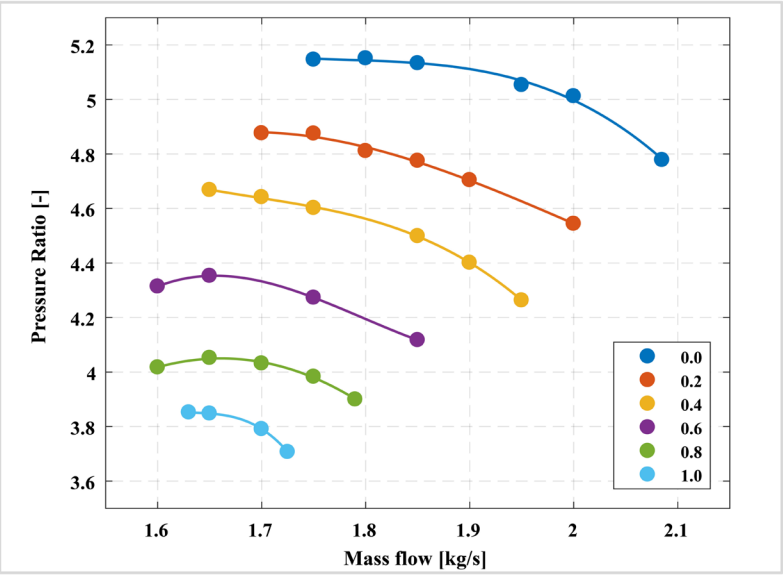

Figure 7. Pressure ratio curves for several tip gap heights.

Investigating the full operating range, it was noticed that the choking mass flow rate varies linearly with tip gap height (**Figure 8**).

Finding a reliable correlation to predict the curve slope could be an important tool in preliminary design steps in order to understand the correct tip gap scaling; in particular, the upper limit beyond which the design mass flow cannot be processed which is strongly related to manufacture technologic requirements.

4.2.2. Flow Field Analysis

In order to better understand the effect of tip gap height on flow field main parameters and thus on overall performance of the machine, a detailed investigation of significant quantities and flow properties was performed. One of the most interesting section on which analyze these quantities is the impeller outlet section (corresponding also to diffuser inlet section), highlighted in cyan in **Figure 9**.

For this section, several color contour representations are reported in the following figures, representing two flow passages, each one constituted by a splitter blade and a main blade, in this order from left to right. In order to compare similar cases for each operating condition, the best efficiency point for each performance curve is considered. Thus, the mass flow rate changes for each represented condition, as reported in **Table 2**, where three significant cases are listed.

In **Figure 10** the color contour of total to total pressure ratio is reported. It is necessary to remember that this compression ratio is the one calculated downstream of the rotor, therefore it will be lower than the global one shown in **Figure 7**. The rotation direction is indicated with ω. As attended, according to performance curves of **Figure 7**, the overall value decreases with the increasing of impeller tip gap height. For all the investigated cases, lower values of total to total pressure ratio are located downstream the splitter and main blade trailing edges. As expected, β_{tt} is lower downstream of splitter blades trailing edges

with respect to main blade ones, due to the lower compression effect associated to this kind of blades.

Table 2. Analyzed cases.

Case	Tip gap height [mm]	Mass flow rate [kg/s]
a	0.2	1.85
b	0.6	1.75
c	1.0	1.65

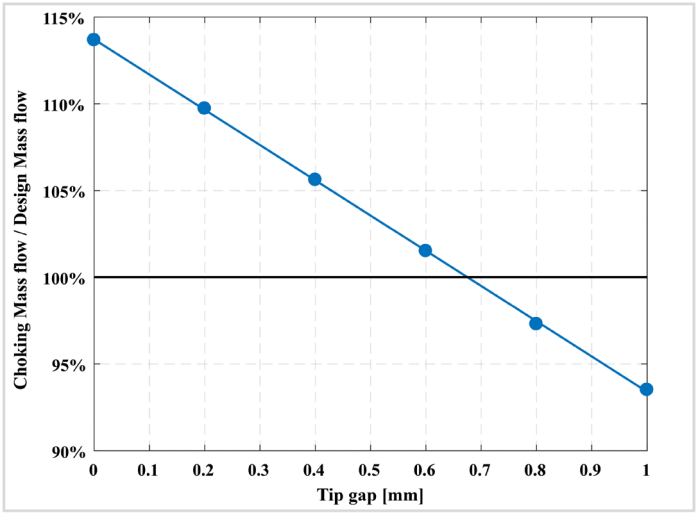

Figure 8. Normalized chocking mass flow rate as a function of tip gap height.

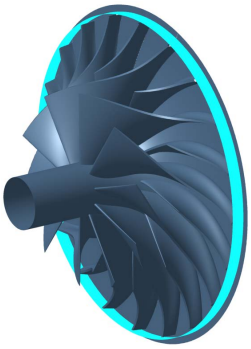

Figure 9. Representation of impeller exit section for flow field evaluation.

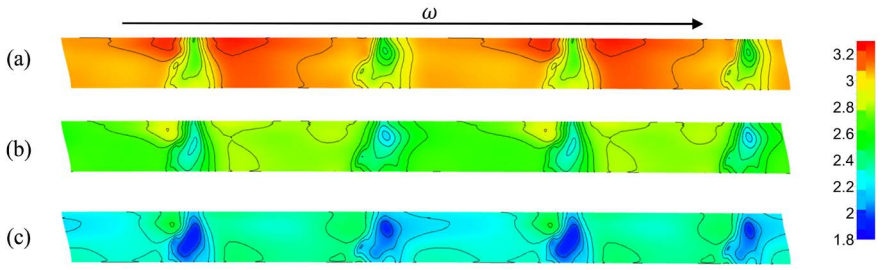

Figure 10. Pressure ratio at rotor exit for 0.2 mm (a), 0.6 mm (b) and 1 mm (c) tip gap height.

In Figure 11, the corrected entropy colour contour is reported. The corrected entropy is calculated in order to make the values obtained from the different operating conditions comparable, referring the quantity to the inlet conditions, indicated with subscripts 0:

$$s_{corr} = \frac{s - s_0}{\frac{w_0^2/2}{T_0}} \tag{3}$$

where w_0 is the inlet relative velocity and T_0 is the inlet temperature. From Figure 11, which represents the corrected entropy for the three studied configurations, it is noticed, as expected, the entropy peaks downstream of the trailing edges of the blades (with peaks of greater intensity downstream of the main blades, due to the greater extension of the blade and therefore of the surface of boundary layer development). Moreover, an increase in the mean value of the corrected entropy, within the channels and within the wakes, with the increase of the tip gap height is highlighted.

Figure 12 shows the colour contours of the absolute flow angle for the three simulated conditions. Considering that the absolute flow angle design value is equal to about 68˚, it can be noticed that for the smallest tip gap height this value is respected within the bladed channel.

On the contrary, as the tip gap increases, in addition to an increase of the value of the angle in the tip leakage area, characterized by an uncontrolled value of the absolute angle of the flow (approaching or exceeding 90˚), the value of the angle within the bladed channel undergoes a strong variation, with values that are reduced, near the hub region, at around 40˚ for the worst case (case c). To compensate the extensive flow blockage induced by the larger tip clearance, the fluid is deflected in the radial direction to preserve the assigned mass flow rate. These strong variations in the absolute flow angle from the design value entail an incorrect operation of the bladed diffuser located downstream of the rotor, with a consequent reduction in the effect of pressure recovery and consequently of the performance of the machine in terms of compression ratio and efficiency, as highlighted in Figure 6 and Figure 7. In Figure 13 and Figure 14 respectively, the color contours of the corrected entropy are shown in the blade to blade sections of midspan and in the span section 0.95 for two bladed channels for the three cases previously illustrated in Table 2.

As can be seen from the trends of Figure 13, the midspan section is influenced not too significantly by the value of the tip gap height, with a modest increase in the corrected entropy in the final zones of the suction side of both the main and the splitter blades, which however remains within the value of the unit. A different situation is instead found in the span section equal to 0.95, *i.e.* located near the tip gap.

In fact, in Figure 14, it can be noticed how the increase in the value of the tip gap height involves significant variations in the corrected entropy field, with significant alterations up to the inlet area of the blade as the height of the tip gap increases. These changes indicate a strong tip leakage flow, and a strong recircu-

lation flow in the area close to the shroud. In order to highlight this phenomenon, a section orthogonal to the axis of the machine in correspondence of the line drawn in the blade to blade sections of Figure 14 is made, obtaining the flow fields shown in Figure 15.

The entropy increase at the inlet highlights the extension of the zone of flow recirculation. The losses are produced in the tip leakage region and are transferred back to the inlet section by the reverse flow.

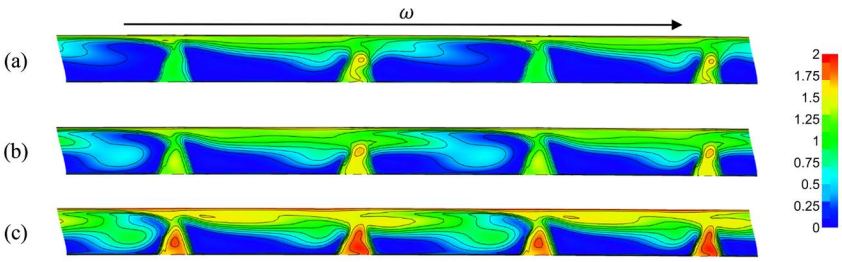

Figure 11. Corrected entropy at rotor exit for 0.2 mm (a), 0.6 mm (b) and 1 mm (c) tip gap height.

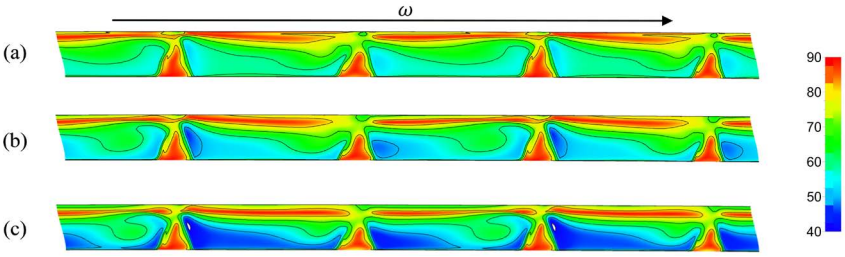

Figure 12. Absolute flow angle at rotor exit for 0.2 mm (a), 0.6 mm (b) and 1 mm (c) tip gap height.

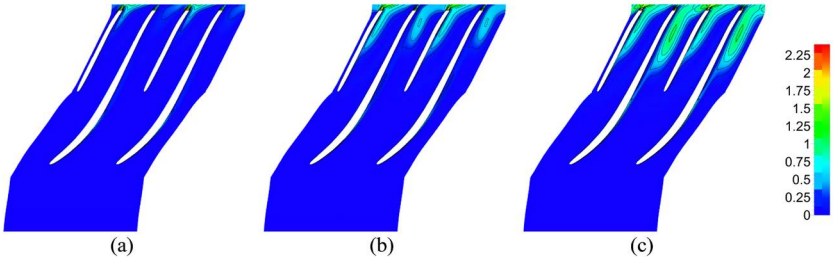

Figure 13. Corrected entropy at midspan section for 0.2 mm (a), 0.6 mm (b) and 1 mm (c) tip gap height.

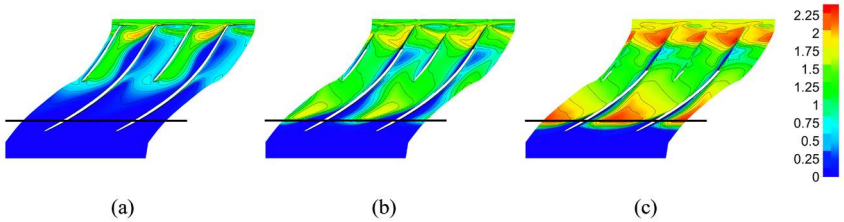

Figure 14. Corrected entropy at span 0.95 section for 0.2 mm (a), 0.6 mm (b) and 1 mm (c) tip gap height.

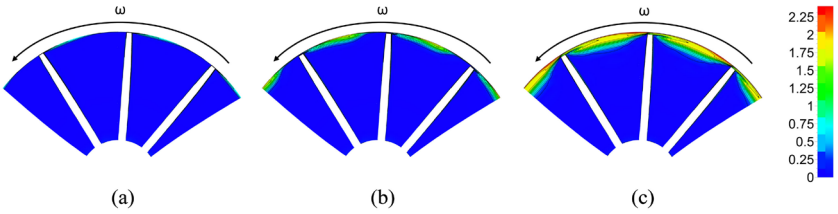

Figure 15. Corrected entropy in orthogonal section for 0.2 mm (a), 0.6 mm (b) and 1 mm (c) tip gap height.

4.2.3. Performance Prediction

A step forward is the prediction of performance variation with the tip gap height through simple one-dimensional equations, accordingly to what is discussed in literature [4]. Starting from thermodynamics relations, the tip leakage flow losses contribution was split in two components: viscous and inviscid losses. The first term is related to the increase of entropy due to the stronger leakage flow when tip gap increases (Entropy effect), while the second one is related to the specific work reduction due to poor guided flow (Work effect). In **Figure 16**, the efficiency drop is presented, in analogy with the article by Eum *et al.* [4]. The efficiency drop is calculated as:

$$\text{Efficiency drop} = \frac{\Delta\eta}{\eta^*} = C_\tau \frac{\Delta\tau}{\tau^*} - C_s \frac{\Delta s - \Delta s^*}{R} \tag{4}$$

where η is the efficiency, τ is the total temperature ratio and all the quantities with superscript * are referred to zero tip gap height. The coefficients C_τ and C_s are defined as:

$$C_\tau = \frac{1}{\beta_{tt}^{*\frac{\gamma-1}{\gamma}}} - \frac{1}{\tau^* - 1} \tag{5}$$

$$C_s = \frac{\gamma-1}{\gamma}\left(1 + \frac{1}{\beta_{tt}^{*\frac{\gamma-1}{\gamma}} - 1}\right) \tag{6}$$

where γ is the heat capacity ratio.

It is evident how the specific work reduction has a negligible effect on efficiency decrease with tip gap, while viscous losses are relevant. The linear pattern is conserved, but the correlation (sum of viscous and inviscid effects) underestimates the efficiency drop compared to CFD simulations. In similar manner, in **Figure 17** the total to total pressure ratio drop is presented. It is calculated as:

$$\text{Pressure ratio drop} = \frac{\Delta\beta_{tt}}{\beta_{tt}^*} = \frac{\gamma}{\gamma-1}\frac{\Delta\tau}{\tau^*} - \frac{\Delta s - \Delta s^*}{R} \tag{7}$$

In this case, the contributions to losses are equally important and the correlation well captures the results provided by numerical computations.

5. Conclusion

Numerical simulations were conducted in order to evaluate the centrifugal

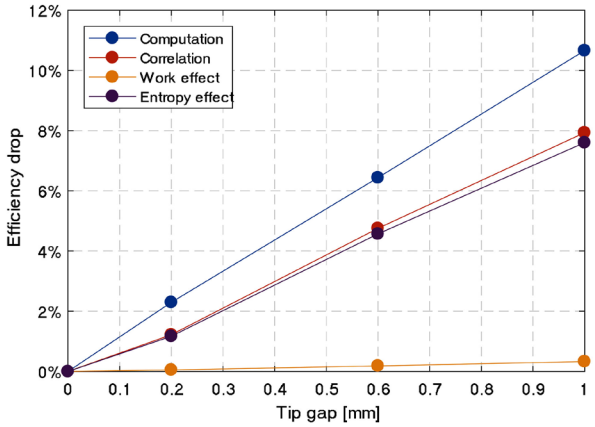

Figure 16. Prediction of efficiency drop as a function of tip gap height.

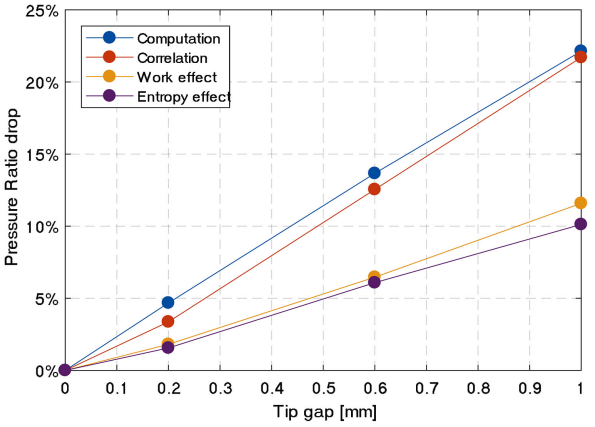

Figure 17. Prediction of total to total pressure ratio drop as a function of tip gap height.

compressor performance variation in scaling process. Global results (e.g. characteristic curves) were justified by detailed analysis on the flow field, with particular attention to the tip gap impact on flow structures. On the one hand, it is noticed that the classical scaling procedure leads to a machine in perfect similarity (velocity triangles, percentage operating range and total to total pressure ratio) with a little increment of efficiency due to the increase in Reynolds number with dimensions. On the other hand, keeping the same tip gap height (same technological limit for impeller manufacturing) has a strong impact on performance, leading to a different machine. Further investigations showed that the variation of tip gap height affects significantly the machine efficiency (up to 10% compared to the ideal case of zero leakage), pressure ratio and operative range extension. In particular, the design mass flow rate cannot be processed if the leakage flow structures are strong enough to obstruct the channel. The study suggests that the global tip gap effect can be determined using simple correlations which relate thermodynamic, aerodynamic and geometrical characteristics. The pattern of efficiency and pressure ratio variation follow the linear behaviour presented in literature, but there are large differences in curve slopes and mismatches in efficiency prediction.

Conflicts of Interest

The authors declare no conflicts of interest regarding the publication of this paper.

References

[1] El-Khattam, W. and Salama, M. (2004) Distributed Generation Technologies, Definitions and Benefits. *Electric Power Systems Research*, **71**, 119-128. https://doi.org/10.1016/j.epsr.2004.01.006

[2] Noman Danish, S., Chaochen, M. and Ce, Y. (2006) The Influence of Tip Clearance on Centrifugal Compressor Stage of a Turbocharger. *Proceedings of the 4th WSEAS International Conference on Fluid Mechanics and Aerodynamics*, Elounda, 21-23 August 2006, 6-11.

[3] Swamy, S. and Pandurangadu, V. (2013) Effect of Tip Clearance on Performance of a Centrifugal Compressor. *IJRET*: *International Journal of Research in Engineering and Technology*, **2**, 447-453.

[4] Eum, H., Kang, Y. and Kang, S. (2004) Tip Clearance Effect on Through-Flow and Performance of a Centrifugal Compressor. *KSME International Journal*, **18**, 979-989. https://doi.org/10.1007/BF02990870

[5] Xiang, J., Schulter, J. and Duan, F. (2015) Effects of Tip Clearance on Miniature Gas Turbines Compressor Performance: A Numerical Approach. Proceedings of 33*rd AIAA Applied Aerodynamics Conference*, Dallas, 22-26 June 2015. https://doi.org/10.2514/6.2015-2412

[6] Head, A. and Visser, W. (2012) Scaling 3-36 kW Microturbines. *ASME Turbo Expo* 2012: *Turbine Technical Conference and Exposition*, *American Society of Mechanical Engineers*, Copenhagen, 11-15 June 2012, 609-617. https://doi.org/10.1115/GT2012-68685

[7] Ma, Y. and Xi, G. (2010) Effects of Reynolds Number and Heat Transfer on Scaling of a Centrifugal Compressor Impeller. *ASME*, *Turbo Expo*: *Power for Land*, *Sea and Air*, **5**, 565-572. https://doi.org/10.1115/GT2010-23372

[8] Perrone, A., Ratto, L., Ricci, G., Satta, F. and Zunino, P. (2016) Multi-Disciplinary Optimization of a Centrifugal Compressor for Micro-Turbine Applications. *Proceedings of ASME Turbo Expo* 2016: *Turbine Technical Conference and Exposition*, Seoul, 13-17 June 2016, V008T23A025. https://doi.org/10.1115/GT2016-57278

[9] Barsi, D., Perrone, A., Ratto, L., Simoni, D. and Zunino, P. (2015) Radial Inflow Turbine Design through Multidisciplinary Optimization Technique. *Proceedings of ASME Turbo Expo* 2015: *Turbine Technical Conference and Exposition*, Montreal, 15-19 June 2015. https://doi.org/10.1115/GT2015-42702

[10] Barsi, D., Perrone, A., Qu, Y., Ratto, L., Ricci, G., Sergeev, V. and Zunino, P. (2018) Compressor and Turbine Multidisciplinary Design for Highly Efficient Micro-Gas Turbine. *Journal of Thermal Science*, **27**, 259-269. https://doi.org/10.1007/s11630-018-1007-2

[11] Dufour, G., Carbonneau, X., Cazalbou, J. and Chassaing, P. (2006) Practical Use of Similarity and Scaling Laws for Centrifugal Compressor Design. *ASME Turbo Expo* 2006: *Power for Land*, *Sea and Air*, Barcelona, 8-11 May 2006, 1131-1140. https://doi.org/10.1115/GT2006-91227

[12] NUMECA (2018) User Manuals, Academic R&D License 2018.

[13] Bourgeois, R., Martinuzzi, R., Savory, E., Zhang, C. and Roberts, D. (2010) Assessment of Turbulence Model Predictions for an Aero-Engine Centrifugal Compressor. *ASME*, *Journal of Turbomachinery*, **133**, Article ID: 011025.